

Relation between the oxidation growth rate of chromia scales and self-diffusion in Cr₂O₃

A.C.S. SABIONI*, A.M. HUNTZ, J. PHILIBERT, B. LESAGE

Laboratoire de Métallurgie Structurale, CNRS, URA 1107, Bat. 413, Université Paris-XI, F-91405, Orsay Cedex, France

C. MONTY

Laboratoire de Physique des Matériaux, CNRS, Bellevue, F-92195 Meudon, France

In most cases, chromia scales are assumed to grow by predominant chromium diffusion. However, results of Atkinson and Taylor indicated that chromium bulk diffusion could not account for the growth rate of chromia scales. Moreover, recent results of Park *et al.* showed that oxygen diffusion in chromia was faster than chromium diffusion. So, at this date, the controlling process of the growth of chromia scales is not elucidated.

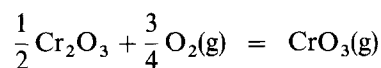
To interpret such a phenomenon, oxygen and chromium self-diffusion coefficients in Cr₂O₃ single crystals and polycrystals were determined in the same materials and in the same experimental conditions, thus allowing a direct comparison. Tracers were introduced by ion implantation, thick film methods, and isotopic exchange, using the ⁵⁴Cr, ⁵⁰Cr and ¹⁸O isotopes. Depth profiling was made by secondary ion mass spectroscopy (SIMS). The bulk diffusion coefficients were computed by using a general solution of the Fick's law taking into account evaporation and exchange at the surface. Grain-boundary diffusion coefficients were computed by using the Whipple–Le Claire equation for type B intergranular diffusion. Lattice and grain boundary self-diffusion coefficients were determined as a function of temperature and oxygen pressure.

The diffusion coefficients are lower than results given in the literature and do not depend on the oxygen pressure. Moreover, it is found that oxygen diffusion is faster than chromium diffusion. These results are compared to the oxidation constants of chromia-forming alloys and it is shown that neither lattice self-diffusion, nor grain-boundary self-diffusion can justify the growth rate of chromia scales. Such a situation is compared to NiO case, for which authors found important differences in grain-boundary diffusivity, according to the elaboration mode of NiO (thermal oxidation or growth from the melt).

1. Introduction

Chromia is an oxide of great technological interest, since it is the major constituent of protective films which grow on stainless steels and many other high-temperature-resistant alloys. Consequently, the literature contains many studies of the formation of chromia scales and of the transport properties of chromia. The growth of chromia scales has been reviewed in a series of articles, first Lillerud and Kofstad, then Hindam and Whittle, Atkinson, and recently Kofstad [1–4]. Above 700 °C, the oxidation kinetics generally obey a parabolic law. A remarkable feature of the parabolic oxidation constants is that they may differ by four orders of magnitude for pure chromium oxidation, and by two orders of magnitude for chromium-bearing alloys [4]. These large differ-

ences may be due to the specimen preparation, and possibly to the evaporation of CrO₃ according to the reaction:



The higher the temperature and the oxygen partial pressure, the more important this evaporation phenomenon.

Whereas it was shown that the chromia growth on pure chromium is dependent on oxygen pressure [1], the parabolic rate constant for chromium-bearing alloys does not depend on the oxygen pressure, in most cases [4]. On the basis of these observations, it could be suggested that chromia scales developed on pure chromium behave as p- or n-type semiconductors,

* Present address: Departamento H de Física, Universidade Federal de Ouro Preto, 35400, Minas Gerais, Brazil

whereas chromia scales developed on Cr-rich alloys behave as extrinsic conductors, due to the presence of doping elements in the scales (see [5], Table 3).

Nevertheless, the microstructural similarities of chromia scales formed on unalloyed chromium and chromia-forming alloys suggest that the same basic growth mechanisms are operative in all cases: outward chromium diffusion is more important than inward oxygen diffusion (materials doped with active elements are not considered here) [4, 6]. These observations agreed with diffusion results obtained some years ago [7, 8]: Kofstad and Lillerud [1] used these earlier data for chromium lattice diffusion to calculate K_p from Wagner's theory and found that the predicted values fall within the range of the measured values. However, in the light of more recent diffusion results, this agreement appears fortuitous: Hoshino *et al.* [9] and Atkinson *et al.* [10] found chromium lattice diffusion coefficients several orders of magnitude smaller than those of the earlier studies, and so too low to account for the rate of oxidation of Cr. They concluded that chromium grain boundary diffusion must be responsible for Cr_2O_3 film growth. Recently, results obtained on cationic and anionic self-diffusion in the bulk and in the grain boundaries of Cr_2O_3 [11, 12] showed that oxygen diffusion in Cr_2O_3 was faster than chromium diffusion.

So, the relative diffusion rate of chromium and oxygen in chromia is not clear and problems remain about the understanding of the growth mechanism of Cr_2O_3 scales on chromium-rich alloys. This is due to the lack of data about the self-diffusion coefficients in dense Cr_2O_3 , particularly for grain-boundary diffusion (only one study is concerned with grain-boundary diffusion), and to the fact that the results obtained for lattice diffusion show a rather important scattering, on account of the difficulties encountered for measuring diffusion coefficients in chromia:

1. It is not easy to obtain dense polycrystals of pure Cr_2O_3 or single crystals of good quality.
2. During heat treatments of chromia in oxygen-controlled atmospheres, it is not certain that equilibrium is reached, due to the low values of the chemical diffusion coefficients [13].
3. Chromium oxide vaporization occurs at high temperature and it is necessary to take this into account when calculating the diffusion coefficients from the concentration profiles [5, 14].
4. Due to the small value of the diffusion coefficients, the penetration depth is very limited and the depth profiling after a diffusion treatment needs accurate procedures [5, 14, 15].

Thus, it appeared necessary to perform new chromium and oxygen self-diffusion experiments on chromia samples of good quality, with an accurate technique for depth profiling, and an appropriate equation taking into account the vaporization phenomena. Such a study is of particular interest if both anion and cation self-diffusion are studied on the same materials, treated in the same conditions. This was our objective: to be able to perform a correct comparison of oxygen and chromium diffusivities and to apply the

results to the interpretation of the growth rate of chromia scales.

2. Experimental

2.1. Material

Cr_2O_3 single crystals [5] of 99.9% purity were provided by Labelcomat (Belgium). Their polished surface for diffusion experiments was parallel to the $(01\bar{1}2)$ plane.

Several attempts were made to obtain dense polycrystals of good quality, by using a high purity powder (impurity < 10 p.p.m): natural high-temperature sintering, HIP and hot-pressing [16, 17]. By sintering, the samples only reached 94% of the theoretical volumic mass, and by HIP, the grain size was small (< 1 μm) and grains pulled out during polishing. Polycrystals prepared by hot-pressing [18] had a volumic mass quite equal to 100% of the theoretical volumic mass of chromia and a grain size of about 9 μm . No grain stripping occurred during polishing. They were used for the grain-boundary diffusion study. All samples were accurately diamond polished and then annealed in atmospheres and temperatures corresponding to the diffusion test conditions.

The ^{54}Cr and ^{50}Cr used as stable tracers and the $^{18}\text{O}_2$ were obtained from CEA (France). Chromium was either deposited by vacuum evaporation as a thick film or ion implanted (CSNSM, Orsay) [5]. For implantation experiments, in a first series, two successive implantations were performed (40 then 100 keV with ion doses of 2.5×10^{16} and 3.8×10^{16} ions cm^{-2} , respectively), and in a second series, samples were implanted with an energy of 150 keV to a dose of 8×10^{16} ions cm^{-2} . Oxygen was introduced either by superficial film or by isotopic exchange [14].

2.2. Diffusion experiments

For chromium diffusion, several series of diffusion experiments were conducted. For lattice diffusion determinations, the diffusion treatments were made first from 1200 to 1450 $^\circ\text{C}$ in an oxygen partial pressure of 5 Pa, and secondly at 1300 $^\circ\text{C}$ from 5 to 3×10^{-8} Pa O_2 [5]. For grain-boundary diffusion determinations, experiments were conducted at 1200 and 1300 $^\circ\text{C}$ in an oxygen partial pressure of 5 Pa [16]. The atmospheres used were Ar or CO_2 -CO mixtures and the oxygen partial pressure was controlled by an yttria-stabilized zirconia gauge.

For the chromium-implanted samples a pre-annealing was performed in the same conditions as for the diffusion treatment [5], and the initial distribution of the tracer was established after this recovery.

For oxygen diffusion [14, 16], most of the experiments were conducted by means of the oxygen exchange method at 1100 $^\circ\text{C}$ in a $p\text{O}_2$ range from 10^{-4} to 1.6×10^{-11} Pa. The atmospheres comprised N_2 - H_2 - H_2^{16}O and N_2 - H_2 - H_2^{18}O mixtures for the pre-annealing and the diffusion treatment, respectively. Sometimes $^{18}\text{O}_2$ -enriched oxygen was used.

A comparative experiment, allowing both oxygen and chromium diffusion coefficients in the same

sample to be directly determined, was made as follows: the stable isotope ^{50}Cr was deposited on the diffusion surface by vacuum evaporation and then oxidized at 700°C for 15 min in an oxygen atmosphere enriched in $^{18}\text{O}_2$ to obtain a $^{50}\text{Cr}_2^{18}\text{O}_3$ superficial film on the sample. Then, the sample was annealed at 1300°C in an oxygen pressure of 3.8×10^{-8} Pa obtained by a CO-CO₂ mixture.

All these experiments allowed us to establish the oxygen pressure and temperature dependencies of chromium and oxygen diffusion in Cr₂O₃.

2.3. Depth profiling

For all experiments, depth profiling was made by secondary ion mass spectroscopy (SIMS) (10 keV Cs⁺ ion source, scanned area of $250 \times 250 \mu\text{m}^2$ and analysed zone of $62 \mu\text{m}$ in diameter) [5]. The penetration depths were obtained by assuming a constant sputtering rate and measuring the final depth of the crater by means of a Talystep profilometer.

2.4. Determinations of the diffusion coefficients

The chromium and oxygen lattice diffusion coefficients were computed by using a general solution of Fick's laws and by taking into account the evaporation and the exchange at the surface [5, 14]. It was verified that the theoretical curves fitted very well with the experimental ones, whatever the method used for introducing the tracer.

For the grain-boundary diffusion experiments [16], the product $D'\delta$ was determined, D' being the intergranular diffusion coefficient and δ being the grain boundary width, by using the Whipple-Le Claire equation for B-type diffusion.

3. Results

3.1. Lattice diffusion coefficients (D) [5, 14]

Figs 1 and 2 are representative of the obtained results on lattice diffusion of chromium and oxygen in chromia as a function of the oxygen pressure and of the inverse of absolute temperature, respectively. The D values are collected in Table I. It can be seen that, for the cationic tracer, there is no difference according to the method used for incorporating the tracer. This indicates, *a posteriori*, that the recovery annealing is sufficient to eliminate the radiation damage and equilibrate the crystal in the implanted zone, and also that the general equations used for computing the diffusion coefficients are adequate.

An example of a profile which clearly shows that evaporation phenomena occur during diffusion is given in Fig. 3. It indicates that vaporization phenomena must be taken into account when calculating the diffusion coefficients, due to the very low penetration depth of tracer during our diffusion treatments. The calculated v values are given in Table I and plotted versus the inverse of absolute temperature in Fig. 4, with literature data for the evaporation rates of chromia. The activation energy of the evaporation,

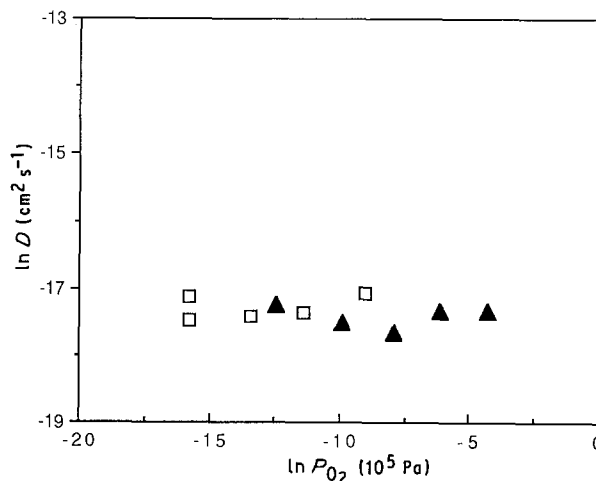


Figure 1 Oxygen pressure dependence of chromium and oxygen bulk diffusion in chromia single crystals, our results. (\blacktriangle) Chromium self-diffusion, 1300°C ; (\square) oxygen self-diffusion, 1100°C .

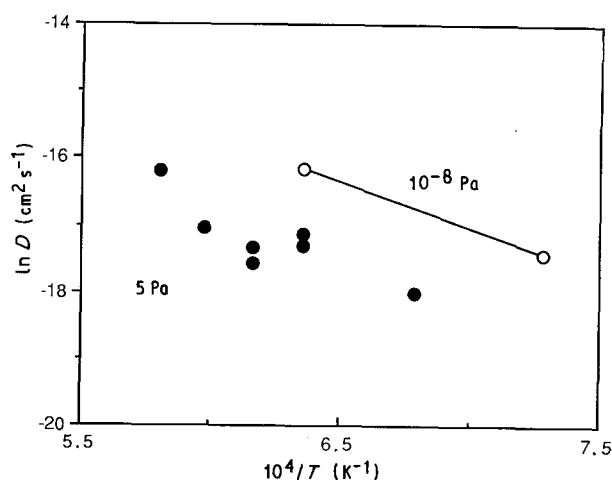


Figure 2 Temperature dependence of chromium and oxygen bulk diffusion in chromia single crystals, our results. (\circ) Oxygen, (\bullet) Chromium.

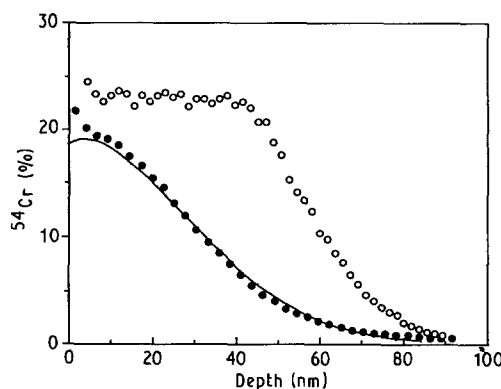


Figure 3 Profiles of ^{54}Cr : (\circ) after implantation and a recovery annealing, and (\bullet) after the diffusion treatment (1300°C , 3.348×10^5 s, 5 Pa O_2), showing that evaporation occurs during the diffusion treatment. (—) Computed fit.

equal to 394 kJ mol^{-1} , is greater than that determined by Hagel ($Q = 204 \text{ kJ mol}^{-1}$) [19] for the loss of Cr₂O₃ due to evaporation.

The comparison of chromium and oxygen penetration in the chromia lattice, for the same sample and

TABLE I Chromium (a) and oxygen (b, 1100 °C) bulk diffusion in chromia: experimental conditions and results. Method: (1), (2) Ion implantation; (3)–(12) thick film

Table Ia

Method	$T(^{\circ}\text{C})$	$P_{\text{O}_2}(\text{Pa})$	$t(10^5 \text{ s})$	$D(10^{-18} \text{ cm}^2 \text{ s}^{-1})$	$V(10^{-12} \text{ cm s}^{-1})$	$H(10^6 \text{ cm}^{-1})$	Observation
(1)	1300	5	3.348	5	9.20	0.160	General implantation profile (two energies) Gaussian implantation profile (one energy)
(2)	1300	5	3.384	7.2 4.9	15 5.5	1.10 1.43	
(3)	1200	5	3.4	1.0	0	0	Calculated from previous profile (9) after a new diffusion annealing
(4)	1300	5	0.7920	4.8	0.5	0	
(5)	1300	6.9×10^{-2}	1.740	4.7	1.15	0	
(6)	1300	1.25×10^{-3}	0.8460	2.2	5.5	0	
(7)	1300	1.26×10^{-5}	1.770	3.1	0.5	0	
(8)	1300	3×10^{-8}	1.908	5.8	5.07	0	
(9)	1350	5	0.7920	4.6	3.0	0	
(10)	1350	5	1.566	2.7	5.575	0	
(11)	1400	5	0.7860	9.0	8.0	0	
(12)	1450	5	0.2340	63	67.3	1.55	

Table Ib

$P_{\text{O}_2}(\text{Pa})$	$t(10^5)$	$D(10^{-18} \text{ cm}^2 \text{ s}^{-1})$	$v(10^{-12} \text{ cm s}^{-1})$	$H(10^5 \text{ cm}^{-1})$
10^{-4}	0.864	8.4	4.9	1.071
$10^{-6.43}$	1.775	4.4	2.2	2.045
$10^{-8.43}$	1.75	3.8	4.22	1.394
$10^{-10.8}$	0.864	7.4	2.7	1.351
$10^{-10.8}$	1.728	3.2	1.78	2.531

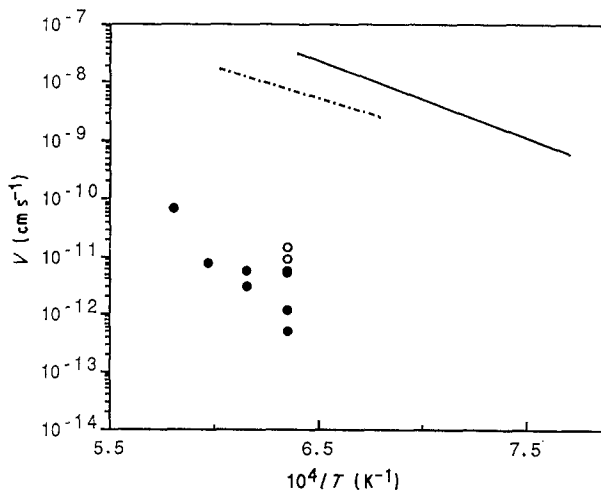


Figure 4 Arrhenius plot of the evaporation rate in chromia: (●) and (○) our results, (thick film deposition and implantation, respectively, both single crystals at $1-10^{-8}$ Pa), (—) Stearns *et al.* results [20], thermally grown Cr_2O_3 , 15 Pa, (---) Hagel's results [19], hot-pressed Cr_2O_3 polycrystal, 10^4 Pa.

the same diffusion conditions, (obtained from the $^{50}\text{Cr}_2^{18}\text{O}_3$ superficial film) is shown in Fig. 5.

3.2. Grain-boundary diffusion coefficients (D') [16]

The results for intergranular diffusion are collected in Table II. Fig. 6 shows the results of self-diffusion of chromium and oxygen in the grain boundaries, as a

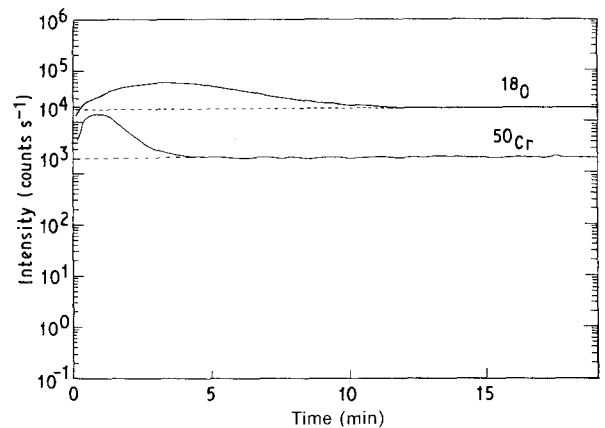


Figure 5 Comparison of chromium and oxygen diffusion profiles in chromia single crystals: SIMS spectra of the ^{18}O and ^{50}Cr isotopes after diffusion at 1300°C in 3.8×10^{-8} Pa oxygen atmosphere.

function of the inverse of absolute temperature, and Fig. 7 shows the dependence of the oxygen grain boundary diffusion on the oxygen pressure.

As an example, in Fig. 8, two profiles obtained for the same tracer, in a monocrystalline sample (lattice diffusion) and in a polycrystalline sample (grain-boundary diffusion), are shown. It clearly appears that the two profiles differ significantly and represent two different diffusion mechanisms. Note also that no diffusion tail appears on the profile relative to lattice diffusion. This was a general finding in our experiments on single crystals.

TABLE II Chromium (a) and oxygen (b) grain-boundary diffusion in chromia: experimental conditions and results. In (b) the second values given for D and $D'\delta$ correspond to an extrapolation of D with pO_2 [16]

Table IIa

$T(^{\circ}C)$	$t(10^4 \text{ s})$	$D(10^{-18} \text{ cm}^2 \text{ s}^{-1})$	$-d \ln c/d \ln x^{6/5} (\text{cm}^{-6/5})$	$D'\delta (\text{cm}^3 \text{ s}^{-1})$	β
1200	6.24	1.0	$2.32/3.21 \times 10^6$	$0.76/1.3 \times 10^{-22}$ $\langle 1.03 \times 10^{-22} \rangle$	206
1300	6.12	4.8	4.33×10^5	4.72×10^{-21}	908
1300	7.92	4.8	6.06×10^5	2.37×10^{-21}	401

Table IIb

$P_{O_2}(\text{Pa})$	$T(^{\circ}C)$	$t(10^4 \text{ s})$	$D(10^{-18} \text{ cm}^2 \text{ s}^{-1})$	$-d \ln c/d \ln x^{6/5} (10^5 \text{ cm}^{-6/5})$	$D'\delta (10^{-21} \text{ cm}^3 \text{ s}^{-1})$	β
2×10^4	1100	8.64	8.4	3.398	7.87	549.8
			200		38.4	23
10^{-4}	1100	8.64	8.4	3.647	7.0	489.2
1.6×10^{-1}	1100	8.64	7.4	6.625	2.4	209.5
			3.2		1.6	474.8

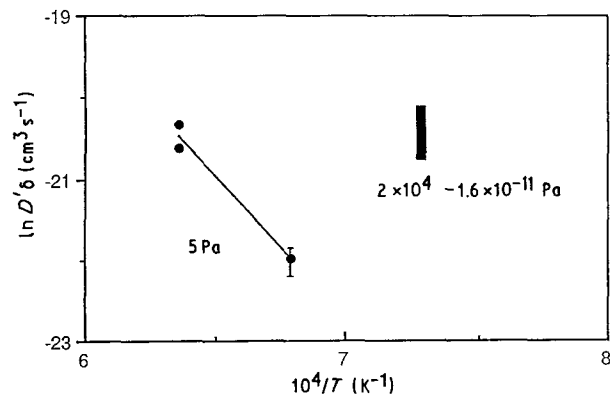


Figure 6 Temperature dependence of chromium and oxygen grain-boundary diffusion in polycrystalline chromia samples, our results. (●) Cr, (■) O.

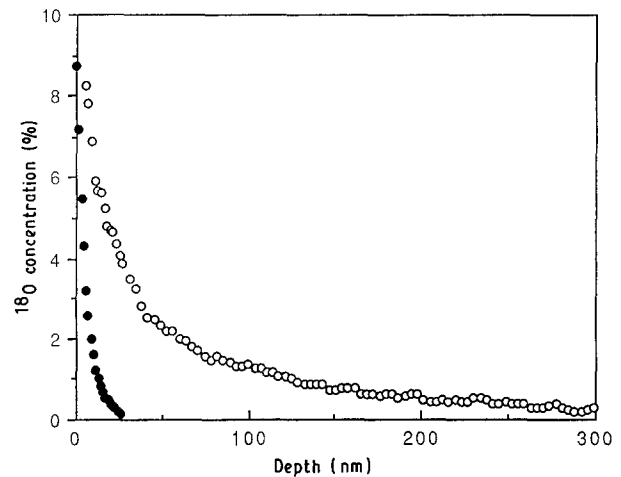


Figure 8 Comparison of oxygen diffusion profiles in a monocrystalline (●) and in a polycrystalline (○) sample ($T = 1100^{\circ}C$, $pO_2 = 10^{-4} \text{ Pa}$, $t = 8.64 \times 10^4 \text{ s}$).

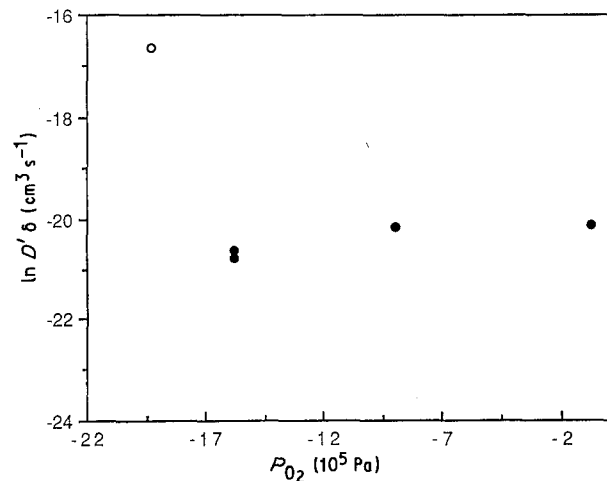


Figure 7 Oxygen pressure dependence of oxygen grain-boundary diffusion in polycrystalline chromia samples, (●) our results, (○) King *et al.* [12]. $T = 1100^{\circ}C$.

4. Discussion

4.1. Evaporation

It can be seen, in Fig. 4, that the evaporation rates determined in this study are much smaller than those

previously given by other authors. According to our penetration depths during diffusion treatments (see Figs 3, 5), if the evaporation rates were of the order of magnitude of those determined by Hagel [19] or Stearns [20], no diffusion profiles would have been obtained. Though negligible when compared to the values of Hagel and Stearns, the evaporation rate v cannot be neglected in our diffusion coefficient calculation. The fact that we obtained smaller v values could be due to the dense character of our chromia samples and to their careful surface preparation to ensure as perfect a surface as possible [5]. Indeed, we observed that the longer the diffusion treatment, the greater the surface degradation and the evaporation rate: for instance, the evaporation rate determined on implanted samples was slightly greater than for samples with thick film due to the fact that the diffusion treatment time chosen for implanted samples must be greater than with the thick film method. Another parameter, which must decrease the evaporation rate

in our experiments, consists in the fact that our samples are in a confining atmosphere.

4.2. Lattice self-diffusion

When comparing our chromium bulk self-diffusion results with those given in the literature (Fig. 9), it is clear that our diffusion coefficients are lower than those previously determined. Already, Hoshino and Peterson [9] and Atkinson and Taylor [10] found that Cr diffusion coefficients were about five orders of magnitude lower than those found by Hagel *et al.* [7] and Walters *et al.* [8]. They consider the data of Hagel *et al.* (obtained on polycrystals), as being related to grain-boundary diffusion, and those of Walters *et al.* (obtained on single crystals), as being due to the effect of dislocations. Our values, obtained on single crystals are still lower. Their reliability is supported by their reproducibility and accuracy. For instance, for one sample treated at 1300 °C, the value of the chromium diffusion coefficient found from a first profile was $D = 7.2 \times 10^{-18} \text{ cm}^2 \text{ s}^{-1}$, and from the profile established on another crater of the same sample, $D = 4.9 \times 10^{-18} \text{ cm}^2 \text{ s}^{-1}$. Moreover, values obtained from two different types of implanted profiles or by thick film deposition are of the same order of magnitude (see Table I).

The difference between our chromium bulk diffusion results and those of Hoshino *et al.* [9] or Atkinson *et al.* [10] could be due to differences in the purity of the single crystals. But, it must be noted that Park *et al.* found the same D value as Atkinson by working on chromia samples containing a great amount of impurity (10000 p.p.m.). So, the most important parameter explaining the obtained differences may be found in the fact that a diffusion tail was never observed in our various profiles, as it was in Atkinson and Taylor's experiments. That eliminates the possibility of short-circuit effects by dislocations or microcracks, in our case. If a chromium concentration profile is calculated by using the general equation and taking for D the value determined by Atkinson *et al.*

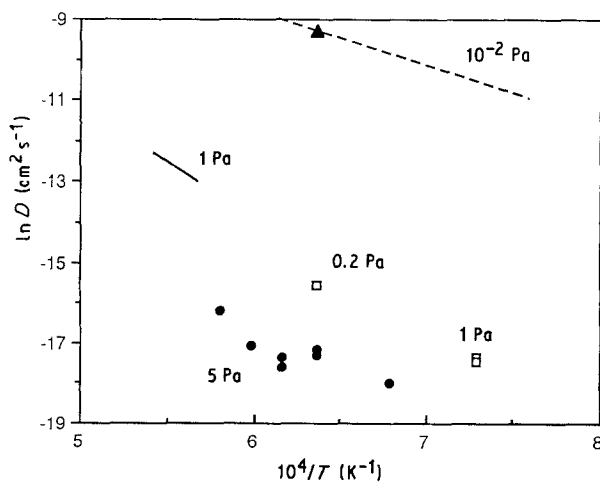


Fig. 9 Comparison with literature data of the chromium bulk self-diffusion in chromia: (●) our results, (□) Atkinson and Taylor [10], (—) Hoshino and Peterson [9], (---) Hagel and Seybolt [7], (▲) Walters and Grace [8].

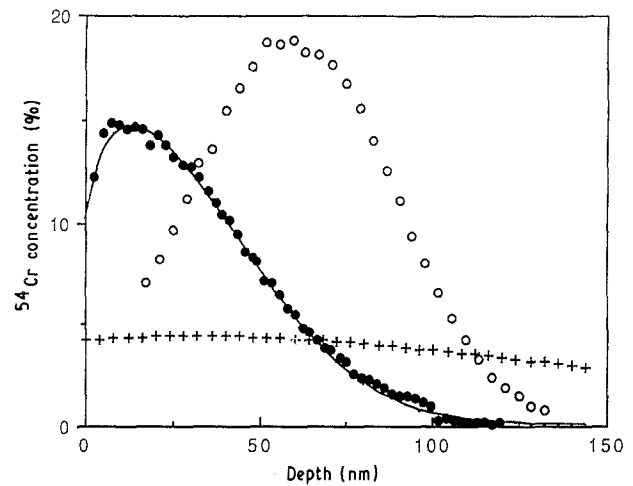


Figure 10 Chromium concentration profiles obtained in one of our experiments (●) and calculated (+) according to the equation used in this study by taking the bulk diffusion coefficient determined at the same temperature by Atkinson *et al.* [10]. (○) Initial profile, (—) theoretical fit ($T = 1300 \text{ °C}$, $t = 3.382 \times 10^5 \text{ s}$, $p\text{O}_2 = 5 \text{ Pa}$).

(Fig. 10), it clearly appears that such a chromium penetration is far from our penetrations.

The same analysis may be made for oxygen bulk diffusion: our oxygen diffusion coefficients are smaller than those found by Hagel [21] or by King *et al.* [11]. But, these last authors worked on polycrystals and their results concerning lattice diffusion are probably distorted due to the fact that they determined their diffusion coefficients in conditions where $(Dt)^{1/2}$ is lower than the sample roughness. In the case of Hagel, their samples were not really monocrystalline and contained up to 5% porosity.

Again, the reliability of our oxygen bulk self-diffusion values, obtained on single crystals are supported by the reproducibility of our measurements [14]. Also in this case a diffusion tail was never observed.

The activation energy of the chromium bulk diffusion in chromia is equal to 280 kJ mol^{-1} . As discussed in [5], due to the impurity content in our samples (1000 p.p.m.), it can be suggested that *extrinsic diffusion* occurs and the activation energy could be equal to the migration enthalpy of the defect responsible for the diffusion.

4.3. Grain boundary diffusion

It also appears that the oxygen and chromium grain-boundary self-diffusion coefficients determined in this study are smaller than the few results given in the literature [11, 12] (Figs 7 and 11). This was discussed in [16], and it was suggested that this difference was mainly due to the difference between the bulk diffusion coefficients D determined in our studies and by the mentioned authors. The same remark is valid for the comparison between our D' values and the diffusion coefficients in dislocations determined by Atkinson *et al.* [10]. The differences in the impurity amount between the chromia samples used in these three studies do not seem to have a major effect.

Though the number of experimental points is limited, an activation energy for the chromium grain-

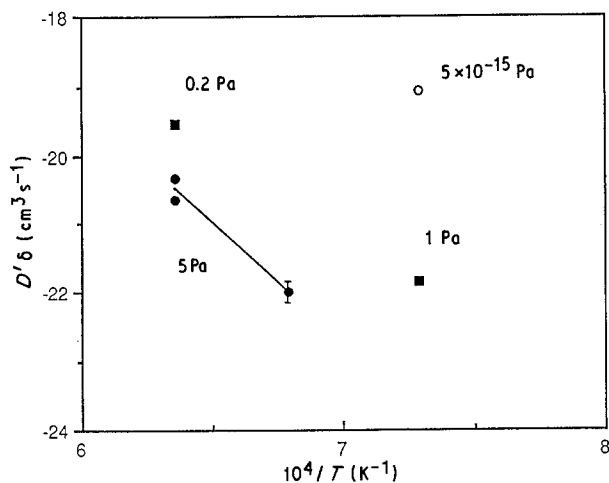


Figure 11 Comparison with literature data of the chromium grain-boundary self-diffusion in chromia: (●) our results, (■) Atkinson and Taylor [10], (○) Park *et al.* [11].

boundary diffusion in chromia was tentatively calculated, and was 675 kJ mol^{-1} . This value is very much greater than the activation energy determined for the chromium bulk diffusion. This difference could be explained by assuming that the impurities, even at a low amount (10 p.p.m.), segregate in the grain boundaries. It must be noted that Prot *et al.* have already found, in alumina, that Q_d (the activation energy of self-diffusion in dislocation walls), and Q_{gb} (the activation energy of self-diffusion in the grain boundaries), were greater than Q [22, 23].

4.4. Oxygen pressure dependence

Our results do not show any dependence of the bulk diffusion coefficients on the oxygen pressure (Fig. 1). The more probable explanation is that extrinsic diffusion occurs, due to the impurity content in our chromia samples (≈ 1000 p.p.m.). The same behaviour was observed for grain-boundary diffusion: though the investigated pO_2 range was large, an oxygen pressure dependency does not appear (Fig. 7).

4.5. Comparison with oxidation rate

In the bulk as in the grain boundary, it is observed that oxygen diffusion is faster than chromium diffusion (see Figs 2, 6 and particularly 5). The results shown in Fig. 5, which were obtained on the same sample, give a direct comparison of chromium and oxygen diffusion in chromia. Such a result appears to contradict the conclusions drawn from oxidation experiments on chromia-forming alloys [1–4, 6, 24], but, as will be seen, other differences concerning transport in chromia are observed between massive chromia samples and chromia scales.

It is possible, on the basis of our self-diffusion results, to calculate the oxidation parabolic constant K_p of chromia scales and to compare it with the literature data on K_p values given by oxidation experiments. Using the Wagner's theory (25), it can be

written:

$$K_p = \int_{pO_2(i)}^{pO_2(e)} (1.5D_{Cr}(\text{eff}) + D_O(\text{eff})) d \ln pO_2$$

where $D_{Cr}(\text{eff})$ and $D_O(\text{eff})$ are the effective diffusion coefficients of chromium and oxygen respectively, with

$$D(\text{eff}) = (1 - f)D + fD'$$

where D is the bulk diffusion coefficient, D' is the grain boundary diffusion coefficient, $f = 2\delta/\Phi$ is the fraction of atoms which diffuse along grain boundaries, with δ the conventional grain boundary width, and Φ the grain size ($\approx 1 \mu\text{m}$).

According to the results of Atkinson *et al.* for Cr lattice diffusion and of Park *et al.* for chromium grain-boundary diffusion, it appears that Cr diffusion in Cr_2O_3 could not be responsible for the growth of chromia scales at 1100°C . Our results are still lower than those of these authors. Thus chromium diffusion can be neglected and K_p is given by

$$K_p = \int_{pO_2(i)}^{pO_2(e)} D_O(\text{eff}) d \ln pO_2$$

Experiments showed that $D_O(\text{eff})$ does not depend on pO_2 , as neither D nor D' vary with the oxygen pressure. In such a case, and using the average value determined in this study at 1100°C for the bulk diffusion and the grain boundary diffusion, i.e. $D = 5 \times 10^{-18} \text{ cm}^2 \text{ s}^{-1}$ and $D'\delta = 5 \times 10^{-21} \text{ cm}^3 \text{ s}^{-1}$, a value is obtained:

$$K_p = 4.5 \times 10^{-15} \text{ cm}^2 \text{ s}^{-1}$$

Note that the oxygen lattice diffusion is also negligible: $D_O(\text{eff})$ is equal to $10^{-16} \text{ cm}^2 \text{ s}^{-1}$.

As shown in Fig. 12, this K_p value is much smaller than K_p values determined by oxidation experiments.

Nevertheless, by considering Figs 9 and 11, it could be suggested that both D and $D'\delta$ vary with the oxygen pressure at low pO_2 , i.e. between $1.6 \times 10^{-11} \text{ Pa}$ (the lowest pO_2 in this study), and $5 \times 10^{-15} \text{ Pa}$, the oxygen pressure of the Cr/ Cr_2O_3 equilibrium at 1100°C .

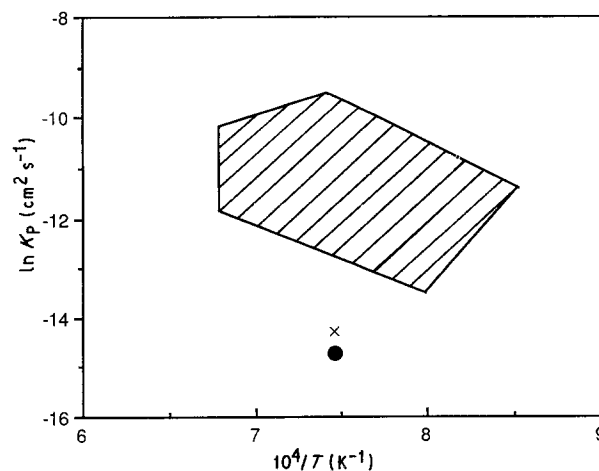


Figure 12 K_p values either calculated from our diffusion results (●) and (×), (×) being the value extrapolated assuming a D variation with pO_2 at low oxygen pressures), or collected from oxidation experiments (streaked area), compiled by King and Park [12].

In such a case, a variation of the diffusion coefficients according to $pO_2^{-1/6}$ could be expected, following a point defect mechanism in lattice and grain boundaries (see [3] and Table 3 of [5]). Assuming such a variation, new values of D and $D'\delta$ were calculated: $D = 1.9 \times 10^{-17} \text{ cm}^2 \text{ s}^{-1}$, and $D'\delta = 1.9 \times 10^{-20} \text{ cm}^3 \text{ s}^{-1}$, respectively. It leads to a new value of the parabolic constant:

$$K_p = 1.75 \times 10^{-14} \text{ cm}^2 \text{ s}^{-1}$$

which is still lower than K_p values determined by oxidation tests (Fig. 12).

On the basis of our diffusion results, it could be suggested that chromia scales grow predominantly by oxygen grain-boundary diffusion. But, according to the calculated K_p value, it appears that even grain-boundary diffusion of oxygen, the fastest diffusion phenomenon in the case of self-diffusion in massive chromia samples, cannot be responsible for the observed oxide growth rates (i.e. for the mass transport). This suggests that grain boundaries can chemically and physically differ according to the elaboration mode of the polycrystals, i.e. polycrystals grown from the melt or obtained by oxidation or by sintering. For instance, the differences in the mass transport rates could be due to a modification of the purity of the scale as its growth is going on. Such a phenomenon was observed during the growth of alumina scales on a FeCrAl alloy [26], and was suggested for NiO scale growth. Another parameter, which can be considered, consists in the fact that, for Cr_2O_3 scale growth, other Cr oxide phases can form before α - Cr_2O_3 nucleates and grows [24]. The crystallinity of the oxide produced by oxidation can also strongly differ, as mentioned by Graham *et al.* (24). Such parameters, and probably others, would explain the discrepancy that has arisen during these past years [27–29] about grain-boundary diffusion coefficients in NiO, for instance.

5. Conclusion

Lattice and grain-boundary diffusion coefficients of chromium and oxygen in Cr_2O_3 single crystals or polycrystalline samples were determined by using stable tracers and depth profiling by SIMS. The diffusion coefficients were studied as a function of temperature (1200–1450 °C) and oxygen pressure ($5\text{--}3 \times 10^{-8}$ Pa).

The diffusion coefficients were computed by using a general solution of Fick's law which takes into account the vaporization phenomena and the exchange at the surface.

For the first time, the chromium and oxygen diffusion coefficients were determined in the bulk and along grain boundaries, on the same materials and in the same conditions.

It clearly appears that it is necessary to consider chromium oxide evaporation for determining available diffusion coefficients. Nevertheless, the evaporation rates of chromia are largely lower than those previously determined.

Chromium and oxygen diffusion coefficients are lower than values previously given in the literature, both in the bulk and in the grain boundaries. Our values of D and D' are representative of lattice and intergranular diffusion, respectively.

Chromium and oxygen diffusion coefficients do not depend on the oxygen pressure, probably on account of an extrinsic diffusion regime.

Oxygen diffusion is faster than chromium diffusion, both in the bulk and in the grain boundaries.

One could think that the growth of chromia scales by oxidation of chromium-rich alloys could be controlled by the faster diffusing species, i.e. oxygen. But, calculations clearly indicate that neither bulk nor grain-boundary diffusion of oxygen can be responsible for the observed growth rate. Other diffusion mechanisms, such as short-circuit diffusion (by microcracks, porosities or channels), should be considered.

More experiments on the growth mechanism of chromia scales would be of great interest.

References

1. K. P. LILLERUD and P. KOFSTAD, *J. Electrochem. Soc.* **127** (1980) 2397; *Oxid. Met.* **17** (1982) 127 and 195.
2. H. HINDAM and D. P. WHITTLE, *Oxid. Met.* **18** (1983) 245.
3. A. ATKINSON, *Rev. Mod. Phys.* **57** (1985) 437–470.
4. P. KOFSTAD, "High temperature corrosion" (Elsevier Applied Science, London, 1988).
5. A. C. S. SABIONI, B. LESAGE, A. M. HUNTZ, J. C. PIVIN and C. MONTY, *Phil. Mag. Part I*, in press.
6. M. J. BENNET and D. P. MOON, "The role of active elements in the oxidation behaviour of high temperature metals and alloys", edited by E. Lang (Elsevier Applied Science, CEC, Petten, 1989).
7. W. C. HAGEL and A. V. SEYBOLT, *J. Electrochem. Soc.* **108** (1961) 1146.
8. L. C. WALTERS and R. E. GRACE, *J. Appl. Phys.* **36** (1965) 2331.
9. K. HOSHINO and N. L. PETERSON, *Bull. Amer. Ceram. Soc.* (1983) C 202.
10. A. ATKINSON and R. I. TAYLOR, *NATO-ASI*, **B 129** (1984) 285.
11. J. H. PARK, W. E. KING and S. J. ROTHMAN, *J. Amer. Ceram. Soc.* **70** (1987) 880.
12. W. E. KING and J. H. PARK, in Conference Proceedings Materials Research Society, Spring Meeting, Reno, Nevada (1988).
13. C. GRESKOVICH, *Comm. Amer. Ceram. Soc.* **67** (1984) C111–C112.
14. A. C. S. SABIONI, A. M. HUNTZ, F. MILLOT and C. MONTY, *Phil. Mag. Part II*, in press.
15. A. ATKINSON, M. L. O'DWYER and R. I. TAYLOR, *J. Mater. Sci.* **18** (1983) 2371.
16. A. C. S. SABIONI, A. M. HUNTZ, F. MILLOT and C. MONTY, *Phil. Mag. Part III*, in press.
17. A. C. S. SABIONI, Doctor Thesis, University Paris XI, Orsay, France, (1990).
18. A. C. S. SABIONI, B. LESAGE, A. M. HUNTZ, J. BESSON, C. DOLIN and C. MONTY, *Colloq. Phys. C* **51** (1990) 611–616.
19. W. C. HAGEL, *Trans. Amer. Soc. Metals* **56** (1963) 583.
20. C. A. STEARNS, F. J. KOHL and G. C. FRYBURG, *J. Electrochem. Soc. Solid State Sci. Technol.* **121** (1974) 945–951.
21. W. C. HAGEL, *J. Amer. Ceram. Soc.* **48** (1965) 70.
22. D. PROT, M. MILOCHE and C. MONTY, *Colloq. Phys. C* **51** (1990) 1027–1033.
23. D. PROT, Doctor Thesis, University Paris VI, France (1991).
24. M. J. GRAHAM, J. I. ELDRIGE, D. F. MITCHELL and R. J. HUSSEY, *Mater. Sci. Forum* **43** (1989) 207–242.

25. C. WAGNER, *Z. Phys. Chem. B* (1933) 21–25.
26. A. M. HUNTZ, G. MOULIN and G. BEN ABDERRAZIK, *Ann. Chim. Fr.* **11** (1986) 291–307.
27. A. ATKINSON, *Mater. Sci. Technol.* **4** (1988) 1046–1051.
28. F. BARBIER and M. DÉCHAMPS, *J. Phys. Coll. C5* **49** (1988) 575–580.
29. F. BARBIER, C. MONTY and M. DÉCHAMPS, *Phil. Mag.* **3** (1988) 475–490.

*Received 8 May
and accepted 12 September 1991*